

## A new hydrodynamic instability in ultra-thin film flows induced by electro-osmosis

Sang W. Joo\*

*School of Mechanical Engineering, Yeungnam University, Gyeongsan 712-749 Korea*

(Manuscript Received March 13, 2007; Revised July 13, 2007; Accepted July 13, 2007)

### Abstract

A new hydrodynamic instability is identified for a nanofluidic flow. The flow analyzed is an electro-osmotic flow of a thin liquid layer, bounded below by a solid substrate and above by an inert gas. The Debye-Hückel approximation is used for the potential distribution, and the interface with the gas is treated as a moving boundary. The stability analysis shows that the flow is always unstable to small-wavenumber disturbances, and the instability is accompanied by interface deformations. Neutral stability bounds due to the capillary cut-off are presented in parametric spaces for the electric field strength and the Debye length of the electrolyte.

**Keywords:** Microfluidics; Instability; Electro-osmosis; Nano; Interface

### 1. Introduction

With recent advances in micro- and nanotechnology, the need to control extremely small amounts of fluids has been acknowledged more strongly than ever. One way to induce and sustain a nano-scale flow is the use of electro-osmosis, as discussed in the monograph by Hunter [1]. Most solid surfaces frequently used in microfluidic devices, such as glass and polymer-based materials, tend to have negatively charged or deprotonated surface chemistries [2]. When a polar liquid layer is placed on such a surface, as in Fig. 1, ions in the liquid are strongly drawn toward the bottom surface and form a very thin layer, called the Stern layer. The ions in this layer are paired with the charges, making the liquid virtually motionless. No flow exists here. Up to some small distance  $\lambda_D$ , called the Debye length, above the Stern layer is the diffuse layer, where excess charges are present. Together these two layers are called the electric double layer (EDL). Above the double layer the

liquid is electrically neutral, and would not react to electric fields. The diffuse layer, however, will, resulting in a nanofluidic flow. Viscous diffusion will then induce a shear flow in the neutral layer. The net flow in these two upper layers is called the electro-osmotic flow.

Many studies of the electro-osmotic flow are done for flows in a channel with width much larger than the Debye length. If a direct-current (DC) electric field is applied parallel to the channel axis, an internal electro-osmotic flow is generated through the channel. As explained by Reppert and Morgan [3], Nguyen and Wereley [2], and Khan and Reppert [4], plug flow develops along the core part of the channel, while a thin shear layer is formed very near the channel wall. At approximately three Debye length ( $3\lambda_D$ ) from the channel wall the fluid reaches the core velocity. In this analysis the Poisson-Boltzmann equation for the electric potential is linearized by the Debye-Hückel approximation due to the small Debye length.

A finite-element simulation using full hydrodynamic equations and the nonlinear Poisson-Boltzmann equation is performed, for example, by

\*Corresponding author. Tel.: +82 52 810 2440, Fax.: +82 52 710 4627  
E-mail address: swjoo@ymail.ac.kr  
DOI 10.1007/s12206-007-1025-6

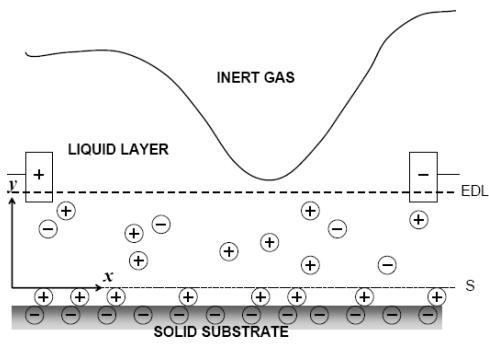


Fig. 1. Configuration of electro-osmotic flow with free surface. Vertical scale is exaggerated: shear line (divides the Stern and the diffuse layer.) EDL: diffusion line (divides EDL and viscous diffusion layer).

Heeren et al. [5], who studied the device-geometry dependence of electro-osmotic flows. Another generalization of the basic electro-osmotic flow includes analyzing the effect of alternating current (AC), known as the frequency-dependent electro-osmosis [4].

In this study we extend the basic electro-osmotic flow to include the effect of interfacial dynamics. The liquid is placed on a substrate with its top surface open to an inert gas phase. The free surface may deform with flow development, and can in turn affect the electro-osmotic flow. This open-channel electro-osmotic flow has many potential applications in nanofluidic devices, such as transportation of specimen in a lab-on-a-chip.

The basic-state flow field is obtained in section 2, and in the ensuing section it will be shown that this flow is always unstable and corrugations on the free surface result.

Although analogous shear-flow instabilities for thin films with free boundaries have been studied extensively before (e.g., Lin and Wang [6]), the one for electro-osmotic flow apparently has not been reported.

## 2. Basic state

We consider a liquid layer of density  $\rho$ , kinematic viscosity  $\nu$ , and mean thickness  $d$  placed on a negatively charged substrate, as shown in Fig. 1. The layer is conceptually divided into three sublayers: the Stern layer (between the bottom and line  $S$  in the figure), the diffuse or Gouy-Chapman layer (between lines EDL and S), and the viscous-diffusion layer (between line EDL and top surface). An electrical field of

strength  $E_{el}$  is imposed parallel to the substrate surface, and a horizontal electro-osmosis flow is induced in the diffuse layer of EDL and in the viscous-diffusion layer. Liquid particles in the Stern layer are assumed immobilized by their pairing with the charges on the substrate. The layer is bounded above by its interface with an inert gas, and so the top surface may deform with flow development.

If we nondimensionalize the system by using  $d, d^2/\nu, \nu/d$  as unit length, time, and velocity, respectively, and denote the horizontal and vertical component of the velocity vector as  $u$  and  $v$ , respectively, the momentum conservation in the horizontal direction is expressed as

$$u_t + uu_x + vu_y = -p_x + u_{xx} + u_{yy} + \frac{E_0}{De^2} e^{-y/De}, \quad (1)$$

where the dimensionless vertical axis  $y$  starts on line  $S$ . Here the pressure  $p$  is in units of  $\rho v^2/d^2$ , and subscripts denote partial differentiations. The last term in Eq. (1) represents the electro-osmotic force, obtained by applying the Debye-Hückel approximation to the Poisson-Boltzmann equation for the electrical potential. This approximation is basically a Taylor-series-expansion linearization of a hyperbolic sine term, and is valid for small Debye length  $\lambda_D$  of the electrolyte, which is defined by

$$\lambda_D = \left( \frac{\varepsilon K T}{2 z^2 F^2 c_\infty} \right)^{1/2} \quad (2)$$

where  $\varepsilon$ ,  $K$ ,  $T$ ,  $z$ ,  $F$ , and  $c_\infty$  are, respectively, the dielectric constant, the Boltzmann constant, absolute temperature, charge number (valence) of each ion, Faraday's constant, and bulk concentration of ions. We define electro-osmosis number

$$E_0 = \frac{\varepsilon E_{el} \zeta d}{\rho v^2} \quad (3)$$

as a measure of the electrical field strength, where the zeta potential  $\zeta$  is the potential at the shear line  $S$ , and is measurable. Another nondimensional parameter

$$De = \frac{\lambda_D}{d} \quad (4)$$

is defined as Debye number, which measures the Debye length relative to the thickness of the liquid layer.

The conservation of vertical momentum and that of mass are unaltered from classical hydrodynamics, and are written as

$$v_t + uv_x + vv_y = -p_y + v_{xx} + v_{yy} \quad (5)$$

$$u_x + v_y = 0 \quad (6)$$

where gravitational acceleration is neglected considering the nano-scale of the fluid.

No-slip boundary conditions are imposed along the shear line S, instead of the bottom plane:

$$u = v = 0 \text{ on } y = 0. \quad (7)$$

The normal component of surface traction across the liquid-gas interface has a jump due to surface tension, which is expressed by

$$\begin{aligned} & -p + \frac{2}{N} [u_x(\eta^2 - 1) - \eta_x(u_y + v_x)] \\ &= \frac{S}{N^3} \eta_{xx} \text{ on } y = 1 + \eta \end{aligned} \quad (8)$$

where  $N = \sqrt{1 + h_x^2}$ , and  $\eta(x, t)$  is the local deflection of the interface from its mean location  $y = 1$ . The dimensionless surface-tension parameter is defined as

$$S = \frac{\gamma d}{\rho v^2} \quad (9)$$

where  $\gamma$  is the surface-tension coefficient. The liquid-gas interface is assumed clean, and so the tangential component of the surface traction vanishes:

$$(u_y + v_x)(1 - \eta^2) - 4u_x\eta_x = 0 \text{ on } y = 1 + \eta \quad (10)$$

The location of the interface is defined by the kinematic condition

$$\eta_t = v + u\eta_x \text{ on } y = 1 + \eta \quad (11)$$

which states that the interface is a material surface.

One set of solutions to the above system represent a unidirectional steady flow with no interface deflection, and are written as

$$\bar{v} = \bar{p} = \bar{\eta} = 0 \quad (12)$$

where the bars denote basic states. The streamwise component of the velocity vector is obtained by solving

$$0 = \bar{u}_{yy} + \frac{E_0}{De^2} e^{-y/De} \quad (13)$$

from Eq. (1), with

$$u = 0 \text{ on } y = 0 \text{ and } u_y = 0 \text{ on } y = 1 \quad (14)$$

We then obtain

$$\bar{u}(y) = E_0 \left( 1 - e^{-y/De} \right) - \frac{y}{De} e^{1/De} \quad (15)$$

It starts at zero on the shear line S( $y = 0$ ), and increases to a maximum

$$\bar{u}_{\max} = E_0 \left[ 1 - \left( 1 + 1 \frac{1}{De} \right) e^{-1/De} \right] \quad (16)$$

on the interface. For small  $De$  the maximum speed is reached very close to the substrate, and a plug flow is generated in most part of the layer. For large  $De$  the speed increases almost linearly. The volumetric flow rate associated with Eq. (16) is

$$\bar{Q} = E_0 \left[ 1 - De + \left( De - \frac{1}{De} \right) e^{-1/De} \right] \quad (17)$$

which varies from  $E_0$  for small  $De$  to  $E_0(1 - 1/(2De))$  for large  $De$ .

### 3. Linear stability analysis

We study the stability of the basic state obtained in the previous section by superposing disturbances of a small amplitude  $\delta$  and wavenumber  $\kappa$  and by writing

$$u(x, y, t) = \bar{u}(y) + \delta [e^{\sigma t + ikx} U(y) + c.c.] \quad (18)$$

$$v(x, y, t) = \delta [e^{\sigma t + ikx} V(y) + c.c.] \quad (19)$$

$$p(x, y, t) = \delta [e^{\sigma t + ikx} P(y) + c.c.] \quad (20)$$

$$\eta(x, t) = \delta [e^{\sigma t + ikx} \Psi(y) + c.c.] \quad (21)$$

where  $\sigma = \sigma_r + i\sigma_i$  is the complex growth rate of the disturbances, and c.c. denotes complex conjugates. In these normal-mode representations the stability of the basic state is determined by the sense of the real growth rate  $\sigma_r$ . If  $\sigma_r > 0$  ( $\sigma_r < 0$ ), the disturbances will grow (decay) in time and the flow is called linearly unstable (stable). The neutral stability bounds are represented by  $\sigma_r = 0$ .

If we substitute the above expressions into Eqs. (1)-(6), linearize the resulting equations in  $\delta$ , and eliminate other dependent variables to compress the system of equations into one for the eigenfunction  $V(y)$ , we obtain

$$\begin{aligned} V^{(iy)} - (2k^2 + ik\bar{u} + \sigma)V'' + ik\bar{u}'V' \\ + k^2(k^2 + ik\bar{u} + \sigma)V = 0 \end{aligned} \quad (22)$$

where the primes denote differentiation in  $y$ . The associated boundary conditions are derived from Eqs. (7)-(11), and are written as

$$V(0) = V'(0) = 0. \quad (23)$$

$$\begin{aligned} V(1) - \frac{\sigma - ik\bar{u}_{\max}}{k^4 S} [V'''(1)] \\ - (3k^2 + ik\bar{u}_{\max} + \sigma)V'(1) = 0 \end{aligned} \quad (24)$$

$$V''(1) + k^2 V(1) = 0. \quad (25)$$

The coefficient  $\Psi$  for the surface deflection is obtained by

$$\Psi = \frac{1}{k^4 S} [V'''(1) - (3k^2 + ik\bar{u}_{\max} + \sigma)V'(1)], \quad (26)$$

which vanishes as the surface tension parameter  $S$  asymptotically approaches infinity. The stability bounds beyond which the disturbances grow ( $\sigma_r > 0$ ) can be obtained by solving the eigenvalue problem (22)-(25) with  $\sigma_r = 0$ . The task then involves seeking solutions to the resulting characteristic equation

$$f(k, \sigma_i, E_0, De, S) = 0 \quad (27)$$

where  $f$  is a complex function. While we fix two of the three parameters  $E_0$ ,  $De$ , and  $S$ , we solve Eq. (27) for a given  $\kappa$  by iterating on  $\sigma_i$  and the remaining parameter to satisfy both the real and imaginary part of Eq. (27).

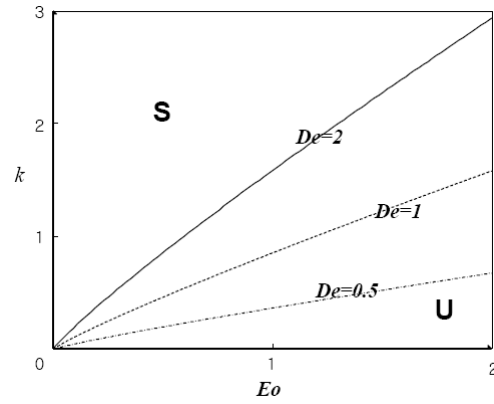


Fig. 2. Neutral stability lines ( $\sigma_r = 0$ ) for  $S = 1$ . Disturbance wavenumber vs. electro-osmosis number.  $S$ : stable region  $U$ : unstable region.

Fig. 2 shows neutral stability curves on the  $\kappa - E_0$  plane for different values of  $De$  with  $S = 1$ . The region below each curve, denoted by the symbol  $U$ , represents the instability. It is noted that for all values of the Debye number  $De$  the instability starts at  $E_0 = 0$ , revealing that the flow is always unstable. For large  $\kappa$  the instability is suppressed by the surface tension, a typical scenario for interfacial instability. As the instability develops, corrugations will develop on the liquid-gas interface possibly in the form of a traveling wave. The instability region increases with  $De$ , and disappears for  $De \rightarrow 0$ .

In Fig. 3 stability bounds are given on the  $\kappa - De$  plane for  $E_0 = 1, 2$  and  $S = 1$ . As is expected from the previous figure, the value of  $\kappa$  for neutral stability approaches zero for  $De \rightarrow 0$ , and increases with the increase of  $De$ . It is noteworthy, however, that  $De \rightarrow 1$  is an unrealistic limit because the thickness of the liquid layers then would have to be much smaller than the Debye length. With the increase in  $E_0$ , the instability region expands without bound.

#### 4. Concluding remarks

A new instability in the open-channel electroosmotic flow is identified by performing a linear stability analysis on the conservation equations with moving boundary conditions. The instability occurs for long-wave disturbances, and accompanies interfacial corrugations. The cut-off value of the electrical field strength for the instability is zero, which shows that all open-channel electro-osmotic flows are unstable regardless of its field strength. The stronger the field strength is relative to the viscous dissipation or

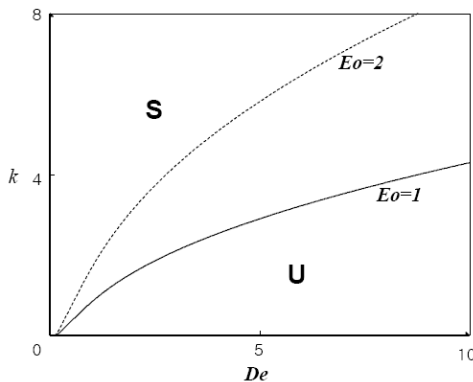


Fig. 3. Neutral stability lines ( $\kappa$  vs.  $De$ ) for  $S = 1$  and  $De = 1, 2$ . S: stable region U: unstable region.

the thicker the Debye length is compared to the thickness of the liquid layer, the more susceptible is the flow to this instability.

Flow developments beyond the onset of the instability identified in the present study can be studied by various nonlinear analyses and by numerical experiments based on the full nonlinear system (1)-(11). Considering the nature of the instability presented here, we expect that the evolution-equation-type approach, used intensively for studies of other hydrodynamic instabilities with long-wave disturbances, becomes a viable choice. This approach will be discussed in a separate note.

### Acknowledgment

This work is supported by the Special Research Grant of Yeungnam University in 2007.

### Nomenclature

$c_\infty$	: Bulk concentration of ions
$d$	: Mean thickness of liquid layer
$De$	: Debye number (dimensionless Debye length)
$E_{el}$	: Strength of electrical field
$E_0$	: Electro-osmosis number (dimensionless electrical field strength)
$F$	: Faraday number
$K$	: Boltzmann constant
$\kappa$	: Disturbance wavenumber
$p$	: Dimensionless pressure
$\bar{Q}$	: Volumetric flow rate in basic state
$S$	: Dimensionless surface-tension parameter

$t$	: Dimensionless time
$u$	: Dimensionless horizontal velocity component
$v$	: Dimensionless vertical velocity component
$x$	: Dimensionless horizontal coordinate
$y$	: Dimensionless vertical coordinate
$z$	: Valence of each ion

### Greek letters

$\delta$	: Linearization parameter
$\varepsilon$	: Dielectric constant
$\gamma$	: Surface tension coefficient
$\eta$	: Interface deflection
$\nu$	: Kinematic viscosity of liquid
$\lambda_D$	: Debye length of the electrolyte
$\rho$	: Liquid density
$\sigma$	: Complex growth rate of disturbance
$\zeta$	: Zeta potential

### Superscripts

'(prime) : Ordinary differentiation in  $y$

### Subscript

$x, y, t$  : Partial differentiation in  $x, y$ , and  $t$

### References

- [1] R. J. Hunter, Introduction to Modern colloid science, Oxford University Press, New York (1996).
- [2] N.-T. Nguyen and S. T. Wereley, Fundamentals and applications of microfluidics, Artech House, London (2002) 54-57.
- [3] P. M. Reppert, F. D. Morgan, Frequency-dependent electroosmosis, *J. Colloid Interface Sci.* (2002) 372-383.
- [4] T. Khan and P. M. Reppert, A finite element formulation of frequency dependent electro-osmosis, *J. Colloid Interface Sci.* 290 (2005) 574-581.
- [5] A. Heeren, C. P. Luo, W. Henschel, M. Fleischer and D. P. Kern, Manipulation of micro- and nanoparticles by electro-osmosis and dielectrophoresis, *Microelectronic Eng.*, in press.
- [6] S.-P. Lin and C.-Y. Wang, Modeling wavy film flows, *Encyclopedia of Fluid Mechanics* 1 (1986) 931-951.